BOREAL ENVIRONMENT RESEARCH 12: 361–373 ISSN 1239-6095
Helsinki 25 June 2007

Modal structure of the atmospheric aerosol particle size spectrum for nucleation burst days in Estonia

Anna Pugatšova, Hilja Iher and Eduard Tamm

Institute of Environmental Physics, University of Tartu, 50090 Tartu, Estonia

Received 31 Oct. 2006, accepted 10 Apr. 2007 (Editor in charge of this article: Veli-Matti Kerminen)

Pugatšova, A., Iher, H. & Tamm, E. 2007: Modal structure of the atmospheric aerosol particle size spectrum for nucleation burst days in Estonia. *Boreal Env. Res.* 12: 361–373.

The modal structure of an atmospheric aerosol size spectrum determines to a significant extent the role of aerosol particles in the formation of weather and climate and their potential danger to living beings. In this paper, the modal structure of the atmospheric aerosol particle size spectra for nucleation burst days was investigated using data acquired at a rural measurement site in Estonia during the year 2005. The measurements were made with the original electrical aerosol spectrometer designed at the Institute of Environmental Physics of the University of Tartu. The performed analysis relied on air mass histories, factor analysis and least-square fitting. The highest particle number concentrations were found in Arctic air masses. The start time of a nucleation burst was found to be dependent on the air mass type: in Arctic air masses nucleation occurred before the noon, whereas in the polar air it occurred in the afternoon.

Introduction

The smallest particles in the atmosphere — secondary particles with the diameters ≤ 20 nm (nanoparticles) — are the product of various gas-to-particle transformation processes: homogeneous and heterogeneous nucleation of gaseous ingredients and the growth of the newborn nuclei by condensation, coagulation and/or chemical reactions on their surface. The above-mentioned transformation processes are, probably, permanently going on with quite a low rate, but the experimental detection of them is very complicated and has not yet been realized just due to this low rate. At some favorable atmospheric conditions, the formation of the nanoparticles occurs with quite a high rate. Such burst-type events of nanoparticle formation have been observed at different places all over the world: at coastal sites (O'Dowd *et al.* 1999, 2002), at suburban (Väkevä *et al.* 2000) and urban (Woo *et al.* 2001, Stainer *et al.* 2002, Kulmala *et al.* 2004a) locations, and in industrialized agricultural regions (Birmili *et al.* 2003).

During recent years, intensive investigations of particle nucleation and growth burst events were performed in European boreal forests (Mäkelä *et al.* 1997, 2000, Kulmala *et al.* 2001, Laakso *et al.* 2004, Vana *et al.* 2004, Dal Maso *et al.* 2005, Vana *et al.* 2006). Here, the most probable nucleation mechanism is the ternary nucleation of water, sulphuric acid and ammonia vapors, whereas the growth to observable sizes (~3 nm) takes place mainly by the condensation of organic vapors (Kulmala *et al.* 2000, 2003, 2004b, Korhonen *et al.* 1999). Ion-induced nucleation can also play an essential role under some conditions (Tamm *et al.* 2001,

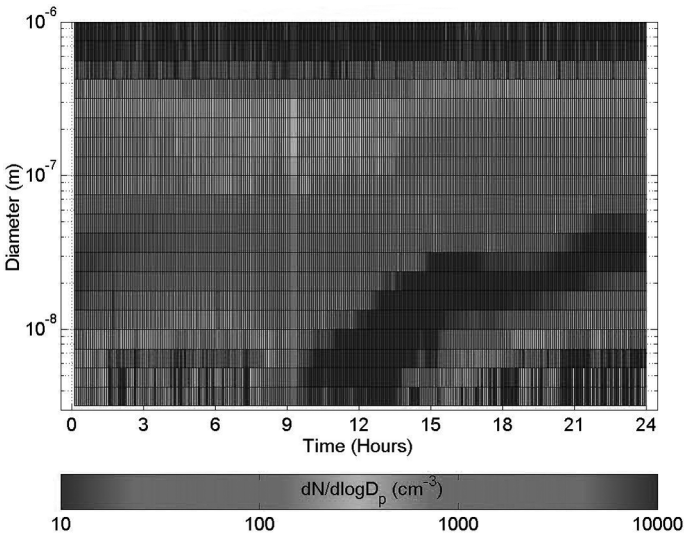

Fig. 1. Surface plot describing atmospheric aerosol spectrum dynamics during the nucleation burst day 8 April 2003. Data were measured with the EAS in Hyytiälä, Finland.

Yu and Turco 2001, Hõrrak *et al*. 2004, Lovejoy *et al*. 2004). These bursts mainly occur due to cold air advection in the polar and Arctic air masses during sunny days after cold nights with temperature inversion. These air masses are usually comparatively clean of accumulation mode particles, so that both the condensation sink of vapours and the coagulation sink of newborn nanoparticles are comparatively low.

The size distribution (SD) of poly-disperse atmospheric aerosol particles can be presented as the sum of a number of lognormal components (modes) (e.g. Whitby *et al*. 1978, Birmili *et al*. 2001, Tunved *et al*. 2003). The modal structure of the SD function and its transformation during the nucleation burst events is of interest for the assessment of the dynamics of particulate air pollution and the formation of cloud condensation nuclei. For the determination of the modal structure of the SD, least-square fitting procedures were used in the above-mentioned and many other papers. The first approximation of the modal particle diameter of these modes was assessed by ocular estimation from the graphs of the SD. Usually, long time series of the measured SDs were analyzed, but the parameters of the modal structure of the SDs were assessed either for each recorded SD or for short-time (e.g. hourly) means. Then these parameters were statistically treated. An example of a typical graphical representation for this type of case study is given in Fig. 1.

In Pugatšova *et al*. (2007) an alternative computation plan was used: a factor analysis was used as a powerful method for the detection of the modes of the long-term mean SD. This plan uses the information carried by the stochastic changes in the particle SD.

In this work, we will analyze the modal structure of the particle SD for the nucleation burst event days by using the data obtained at one measurement point in a rural site of Estonia during one year, and by applying a factor analysis and least-square fitting. Our analysis will be restricted to the Arctic and polar air masses, as these masses are moving to our measurement point mainly from over boreal forest regions. This criterion was used because we will investigate nucleation burst events in Estonia in the Baltic region. In most of the cases considered here, air-masses arrived in Estonia from over boreal forests in Finland. Approximately a half of the Estonian territory is covered by boreal forests as well. In the future, we will compare our results with similar studies in the Nordic countries.

Measurement station and apparatus

Aerosol particle size spectrum in the uniquely wide particle diameter range from 3.2 to 10 000 nm has been measured in Estonia using the original electrical aerosol spectrometer (EAS),

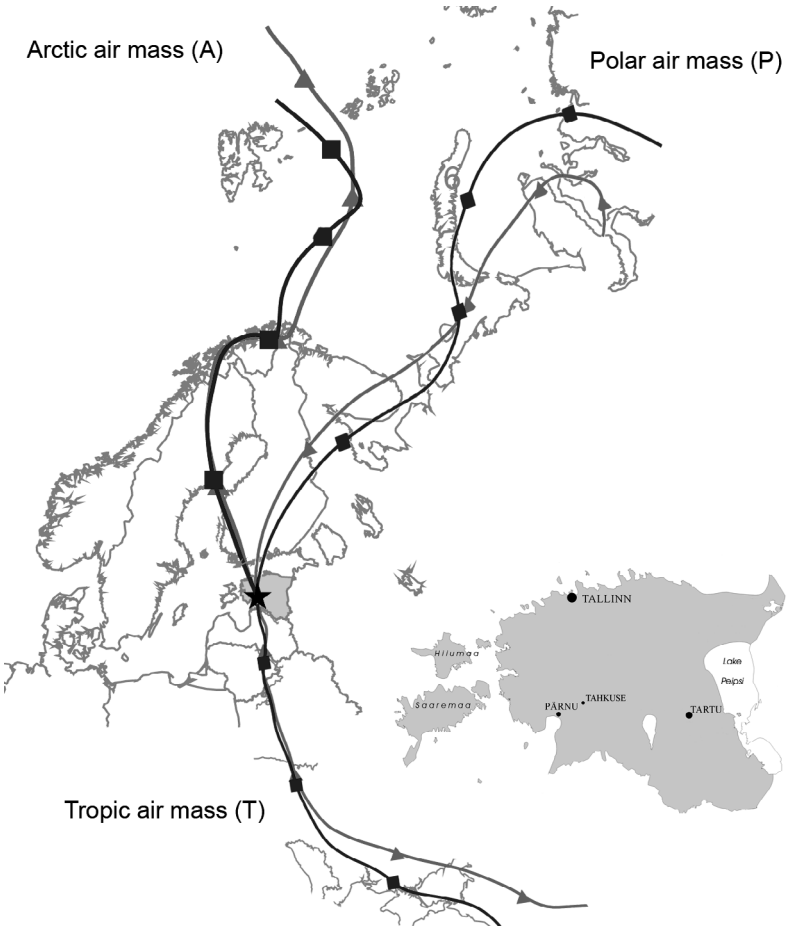

Fig. 2. Examples of air mass trajectories according to the classification 1. The location of the measurement point is marked with a star.

designed at the Institute of Environmental Physics of the University of Tartu (Tammet *et al.* 2002). The mean spectra for each 5 minutes were measured and recorded, totaling in 39 168 recordings during the year 2005. The measurements were performed at the Tahkuse Air Monitoring Station (58°31.5´N, 24°55.5´E, 37 m above the sea level) of the University of Tartu (Fig. 2). This station is located in the southwestern part of Estonia in a rural region with little intensive agricultural activity. More than 50% of the area around the station is covered by boreal forests. The nearest source of air pollution is the small town of Pärnu with 43 000 inhabitants at a distance of 30 km. The measured spectra are presented as a set of 14 number fraction concentrations, the fraction boundaries being uniformly distributed in a logarithmic scale of particle diameter (four fractions per decade). Since the calibration of the first fraction of the old version of the EAS (3.2–5.6 nm in diameter) that was applied is not quite reliable, we used the data of 13 fractions (5.6–10 000 nm).

Nucleation burst day separation

For the separation of days with particle nucleation burst events, we used the number concentration of the first four reliable fractions of the EAS (5.6–10, 10–18, 18–32 and 32–56 nm in diameter). Graphs of the time variations of the number concentrations of these fractions were plotted for all 12 months of year 2005. The days when all four concentrations exceeded 2000 cm^{-3} during some time interval were chosen as days with a nucleation burst event. As a result, we were dealing with quite strong bursts (Vana *et al.*

2006). The analysis presented below is based on data on these nucleation event days only.

Air masses and trajectories

The classification of air masses was done by back-calculating the 96-hour trajectories of air masses arriving at 500 and 1200 m above the model ground level. The trajectories were calculated using the atmospheric model HYSPLIT (Draxler and Hess 1997, 1998) and archive of the meteorological database NOAA (National Oceanic and Atmospheric Administration, http://www.noaa.gov). At first, the air masses were classified according to the standard meteorological classification (classification 1). On the basis of this classification, the air masses were divided into Arctic (A), polar (P) and tropical (T). Another classification (classification 2) was made on the basis of the climatic regions over which the air mass trajectories ran (Vana *et al*. 2002). In this manner, the air masses were classified as modified maritime (MM), modified continental (MC) and pure continental (PC). Pure maritime air masses cannot reach Estonia.

According to the presented classifications, the considered air masses were divided into seven classes (Table 1). The air mass classes T_MM, T_MC and T_PC were left out of further discussion in this paper.

Data handling and analysis

For data processing, we used the method derived and described in Pugatšova *et al*. (2007).

Structure of data file

The measured data from the year 2005, characterizing the aerosol size spectrum (fraction number concentrations), were collected into a joint data file. The code values describing the characteristics of air masses (the direction of the air mass arrival (classification 1) and the type of the air mass (classification 2) were added into the same data file. Then we extracted the sub-file for burst event days according to Table 1. By processing the data using multivariate statistical methods, such as the method of general components and factor analysis, relations between the characteristics of the size spectrum and air mass were studied.

Principles of factor analysis

The basic factor analysis model is represented as

$$\mathbf{Z} = \mathbf{AF} + \Delta, \tag{1}$$

or in the element form,

$$z_i = \sum_{j=1}^{k} a_{i,j} f_j + \Delta_i, \tag{2}$$

where $\mathbf{Z}$ is a vector of the standardized original variables z_i. $\mathbf{A}$ and $\mathbf{F}$ are the matrices of the factor loadings a_{ij} and the vector of factors f_j, respectively, which are unknown and to be estimated from the analysis. The loadings $a_{i,j}$ represent the correlation coefficients between the standardized variable i and factor j, and Δ is a vector of random residuals Δ_i (Kleinbaum *et al*. 1987, Stevens 1996, Krzanowski 2000). In this analysis, number concentrations for 13 EAS

Table 1. Classification of air masses and the total number of burst event days in these air mass classes.

Abbreviation	Classification 1	Classification 2	Total (days)
A_MM	Arctic	Modified maritime	35
A_MC	Arctic	Modified continental	7
P_MM	Polar	Modified maritime	39
P_MC	Polar	Modified continental	19
T_MM	Tropic	Modified maritime	2
T_MC	Tropic	Modified continental	18
T_PC	Tropic	Pure continental	17

fractions were the original standardized variables, and aerosol multimodal structure components — modes — were the factors.

In this analysis, the most essential factors (mostly 5) were separated. These factors describe the structure of the size spectrum. For clear relation of factors with the original variables (particle fraction concentrations) we used the varimax rotation of factors.

Parameterization of the particle SD

The particle SD, f_N, consists of several (n) lognormal modes (Whitby and Sverdrup 1978)

$$f_N(\log D) = \sum_{i=1}^{n} \frac{N_i}{2\pi \log \sigma_{g,i}} \times \exp\left[-\frac{(\log D - \log D_{g,i})^2}{2\log^2 \sigma_{g,i}} \right] = \sum_{i=1}^{n} N_i f_{N,i}(\log D) \quad (3)$$

Here D is the particle diameter, $f_{N,i}(\log D)$ is the distribution density function of the mode i, normalised to unity. The distribution density function of each mode is characterized by three parameters: the mode number concentration N_i (cm^{-3}), the mode geometric standard deviation $\sigma_{g,i}$ (dimensionless), and the mode geometric mean diameter $D_{g,i}$ (nm). The measured spectrum is presented by m = 13 fraction number concentrations K_j.

The parameters N_i, $D_{g,i}$ and $\sigma_{g,i}$ were estimated with the least-square method (Hussein *et al*. 2005) using an iterative algorithm. By varying the above-mentioned parameters, this algorithm minimizes the function:

$$\Phi(N_i, D_{g,i}, \sigma_{g,i}) = \sum_{j=1}^{m} \left\{ K_j - \sum_{i=1}^{n} N_i \left[F_i(\log D_{j,\max}) - F_i(\log D_{j,\min}) \right] \right\}^2. \quad (4)$$

Here $D_{j,\max}$ and $D_{j,\min}$ are the upper and lower limits of the fraction j of the measured spectrum, respectively, and $F_i(\log D)$ is the cumulative lognormal distribution function of the mode i given by

$$F_i(\log D) = \int_0^{\log D} f_{N,i}(\log D, \log D_{g,i}, \log \sigma_{g,i})\, d(\log D). \quad (5)$$

The approximate initial values of the parameters were chosen as follows: $\sigma_{g,i}$ was defined in the range of 1.5–2.05, N_i was about 10 cm^{-3} and the approximate values of $D_{g,i}$ were defined using the graphs of the factor loadings.

Data processing

The analysis was carried out using classifications 1 and 2. The particle fraction number concentrations were treated as the variables in the factor analysis. The number of the retained varimax-rotated factors was chosen according to the slightly modified Kaiser criterion (eigenvalue of the factors to be > 0.7). The retained factors were interpreted as the lognormally distributed components (modes) of the particle size spectrum (Pugatšova *et al*. 2004, 2007). The factor analysis differentiates the objects according to their similar behaviour, i.e. synchronic fluctuating. Random fluctuations in different parts of an aerosol spectrum were used as a source of information about the modal structure of the spectrum. With the help of graphs that show the factor loadings as the functions of the geometric mean diameter for the particle size fractions, the modal diameter and width of these modes were roughly assessed. Then, using the iterative least-square method, the parameters of the lognormal components were specified to obtain the best fit of the sum of the lognormal components with the measured spectrum. Then, we allowed the shifting of the value of the geometric mean diameter until it stayed between the given boundaries of the mode diameters, which are known from the literature (Withby *et al*. 1978, Kulmala *et al*. 2004a). In order to improve the fitting, in some cases we inserted additional modes. These modes could not been clearly seen from the picture showing the factor loadings, but the graphs of some factor loadings had a local small maximum at this point of the diameter scale.

Table 2. Fitted modal parameters for the air mass classes A_MM, A_MC, P_MM and P_MC.

	A_MM			A_MC			P_MM			P_MC		
	N (cm^{-3})	σ_g	D_g (nm)	N (cm^{-3})	σ_g	D_g (nm)	N (cm^{-3})	σ_g	D_g (nm)	N (cm^{-3})	σ_g	D_g (nm)
Nucleation1	1500	1.50	10	1000	1.50	5.6	100	1.35	5.6	150	1.35	5.6
Nucleation2				1300	1.40	24	1750	1.57	14	1200	1.57	14
Aitken1	5400	1.58	40	4100	1.45	44	5100	1.46	56	5500	1.50	60
Aitken2				950	1.65	120						
Condensation	300	1.40	160	10	1.70	700	50	1.80	240	15	1.85	400
Droplet	5	1.25	560				3	1.90	900	1	1.70	1400
Coarse1	1.6	1.90	900	0.30	3.20	3200	0.25	6	5600	0.40	6	5600
Coarse2	0.50	4.00	2400									

Results and discussion

The analysis was carried out using classifications 1 and 2 to investigate the aerosol SD properties associated with the corresponding air mass classes. Table 2 lists the fitted size distribution parameters (geometrical mean diameter (D_g), geometrical standard deviation (σ_g) and number concentration (N) of modes) corresponding to the air mass classes A_MM, A_MC, P_MM and P_MC.

For all the air mass classes shown in Table 2, a multimodal character of the particle number SD was clearly seen. In case of the air mass class A_MM (Fig. 3), we can suppose from the graph of the factor loadings that the SD had a four-modal structure. However, for the fitting of the measured SD with the sum of lognormal modes, two more modes had to be inserted. Factors 4 and 3 correspond to the nucleation and Aitken modes, respectively. Splitting of the accumulation mode into the condensation and droplet mode (Meng and Seinfeld 1994), or splitting of the coarse mode into two sub-modes, could barely be guessed from the graph of the factor loadings. The presented results show that the number concentrations of the first two modes essentially exceeded those of the other four modes, which testified to the presence of nucleation. In case of the air mass class A_MC (Fig. 4), we could see a similar situation: four clear factors but six modes. Here, the accumulation and coarse modes were highly correlated, corresponding to factor 1. Splitting of the Aitken mode was clearly seen (factors 2 and 4), and a nucleation mode 1 had to be inserted for the fitting. The total number concentrations of both nucleation modes were much higher than the number concentration of the nucleation mode in case of the air mass class A_MM. The total number concentration of the Aitken mode was comparable to that in case of the air mass class A_MM (Table 2).

The results described above show clearly the variability of the properties of the SD within similar, yet not identical, air-mass classes.

In case of the air mass classes P_MM (Fig. 5) and P_MC (Fig. 6), a five-modal structure of the SD was clearly seen in the picture of factor loadings, and the fitting procedure required inserting one more factor. The nucleation mode was split

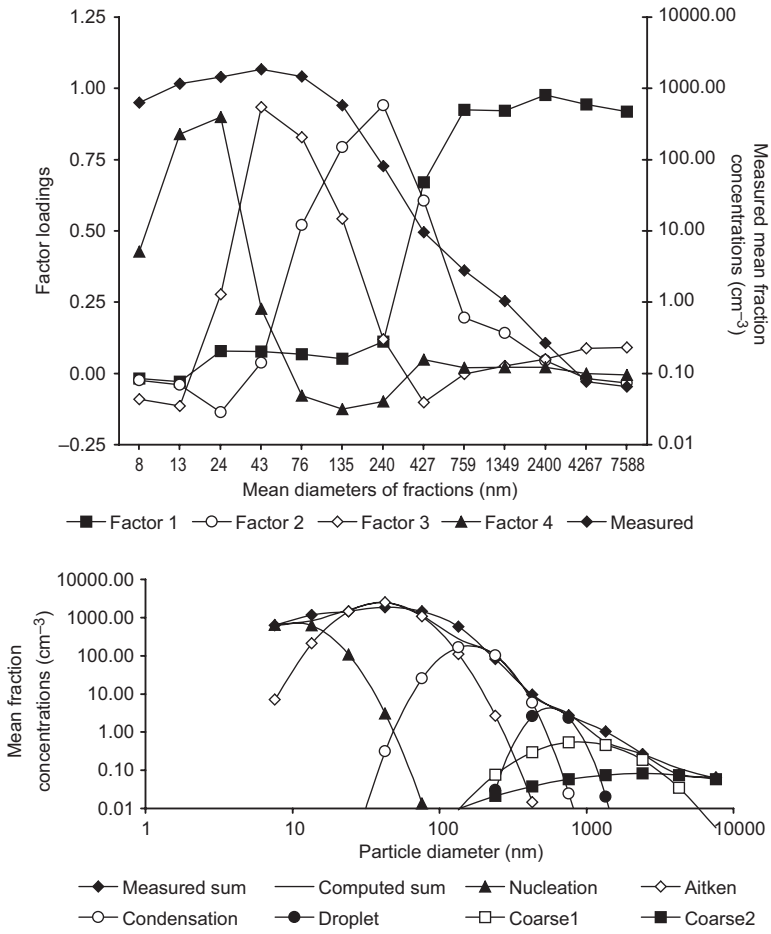

Fig. 3. Factor loadings and measured mean fraction concentrations as a function of mean particle diameter of the fraction (upper graph) for the air mass class A_MM. The lower graph shows the fitted spectrum components (modes), their sum and measured fraction concentrations as a function of particle diameter.

into two sub-modes, while the Aitken mode was not. In both cases, the number concentration of the Aitken mode was much higher than the total number concentration of the nucleation modes (Table 2). The condensation sub-mode of the accumulation mode was clearly seen (factors 2 or 4 in the air mass classes P_MM, P_MC and P_MM (Fig. 4) and P_MC). Factor 1 corresponds to two highly-correlated modes. In Table 2 these modes are indicated as the droplet and coarse mode, but they can also be sub-modes of a split coarse mode.

The above results show that the number concentration of the nucleation mode was lower than that of the Aitken mode. This is due to the fact that the analysis was based on daily-average data. In order to obtain a more detailed picture, we analyzed separately the data corresponding to two different time intervals: that of nucleation and initial growth and that after these processes. Since nucleation bursts started practically always before the noon, we considered separately the time intervals 07:00–13:00 and 13:00–18:00 of the burst event days.

In case of the air mass class A_MM, the number concentration of the nucleation mode was much higher during the first (nucleation and initial growth) time interval than during the second time interval, whereas the number concentration of the Aitken mode was higher in the second time interval. We also found that the Aitken mode was split into three modes during the second time interval with high total number concentrations (Table 3).

The results for the air mass class A_MC (Table 4) show that nucleation occurred around noon or in the afternoon, because the concentration of the nucleation mode was higher after

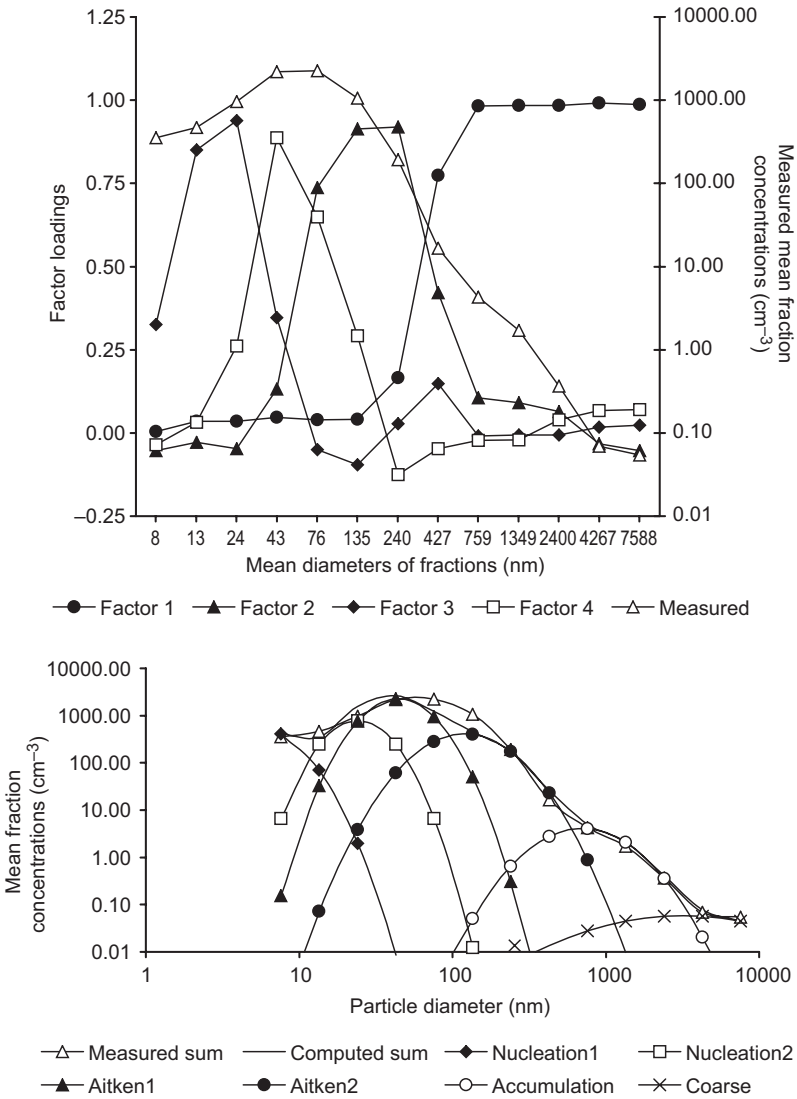

Fig. 4. Factor loadings and measured mean fraction concentrations as a function of mean particle diameter of the fraction (upper graph) for the air mass class A_MC. The lower graph shows the fitted spectrum components (modes), their sum and measured fraction concentrations as a function of particle diameter.

Table 3. Fitted modal parameters for the air mass class A_MM and for two periods (07:00–13:00 and 13:00–18:00).

	07:00–13:00			13:00–18:00		
	N (cm^{-3})	σ_g	D_g (nm)	N (cm^{-3})	σ_g	D_g (nm)
Nucleation	2527	1.58	13.2	1200	1.14	10
Aitken1	4263	1.55	44	4000	1.65	18
Aitken2	600	1.42	136	2569	1.31	56
Aitken3	–	–	–	1333	1.48	98
Condensation	10	1.35	460	8	1.48	570
Droplet	2	1.60	1000			
Coarse	0.50	4.00	2400	0.50	2.50	1900

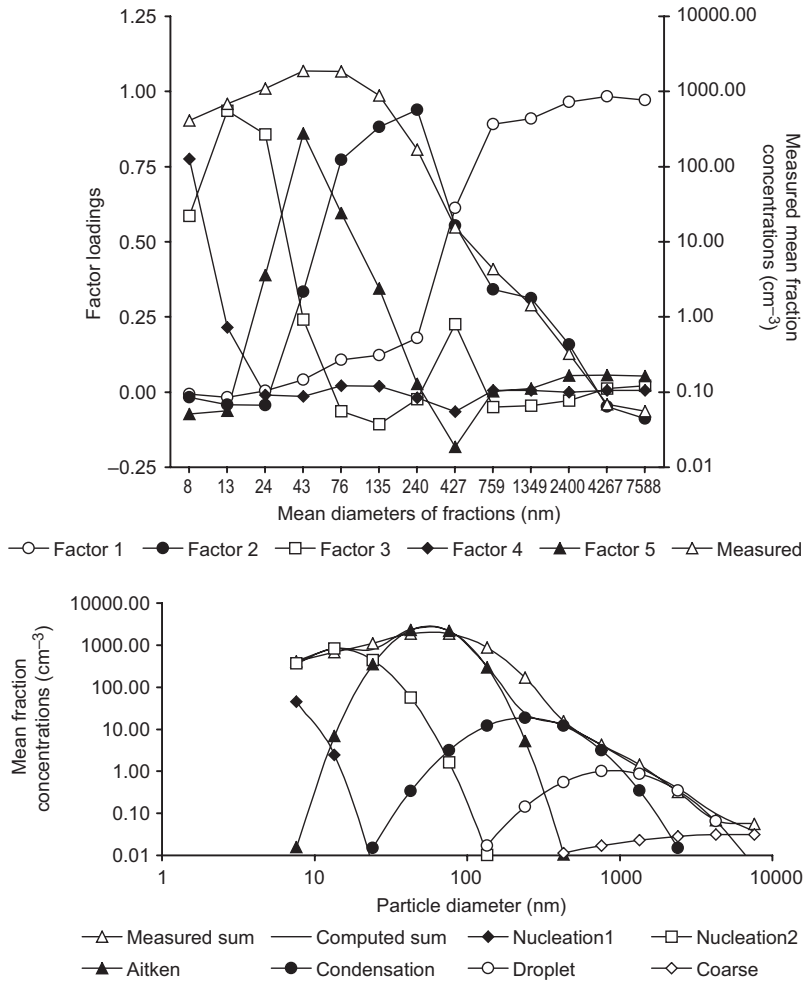

Fig. 5. Factor loadings and measured mean fraction concentrations as a function of mean particle diameter of the fraction (upper graph) for the air mass class P_MM. The lower graph shows the fitted spectrum components (modes), their sum and measured fraction concentrations as a function of particle diameter.

midday compared with the morning. We also see the splitting of the Aitken mode into three submodes with high number concentrations, as in case of the air mass class A_MM.

In case of the air mass classes P_MM and P_MC (Tables 5 and 6), the nucleation burst occurred in the usual time window: in the morning the number concentration of the nucleation

Table 4. Fitted modal parameters for the air mass class A_MC and for two periods (07:00–13:00 and 13:00–18:00).

	07:00–13:00			13:00–18:00		
	N (cm^{-3})	σ_g	D_g (nm)	N (cm^{-3})	σ_g	D_g (nm)
Nucleation1	700	1.30	6	2000	1.49	5.6
Nucleation2	–	–	–	1168	1.30	18
Aitken1	2000	1.56	23	4294	1.38	44
Aitken2	5031	1.38	74	2000	1.49	100
Condensation	50	1.75	240	8	1.60	840
Droplet	5	1.74	880			
Coarse	0.3	4.00	5600	0.30	4.00	5600

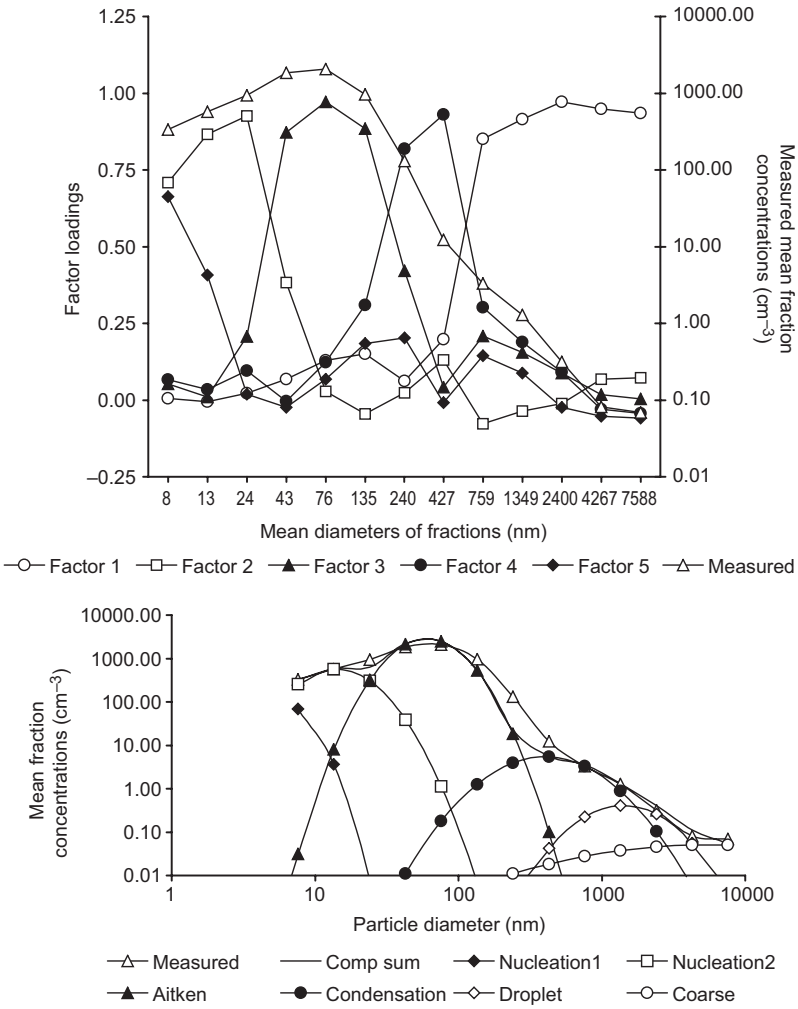

Fig. 6. Factor loadings and measured mean fraction concentrations as a function of mean particle diameter of the fraction (upper graph) for the air mass class P_MC. The lower graph shows the fitted spectrum components (modes), their sum and measured fraction concentrations as a function of particle diameter.

mode was higher than in the afternoon, whereas the number concentration of the Aitken mode was higher in the afternoon. The data of Tables 2–6 show clearly that the modal structure of the particles SD depends essentially on the prehistory of air masses.

For comparison of the particle SD for nucleation burst days and non-burst days, we calculated

Table 5. Fitted modal parameters for the air mass class P_MM and for two periods (07:00–13:00 and 13:00–18:00).

	07:00–13:00			13:00–18:00		
	N (cm^{-3})	σ_g	D_g (nm)	N (cm^{-3})	σ_g	D_g (nm)
Nucleation	2300	1.48	10.6	705	1.50	5.6
Aitken1	4200	1.45	44	2447	1.60	22
Aitken2	–	–	–	4200	1.60	79
Condensation	700	1.64	134	20	1.75	400
Droplet	5	2.25	560	1	1.85	1300
Coarse	0.3	4.00	3200	0.2	3.80	4400

the mean modal structure of the SD for non-event days in case of the air mass class A_MM. The results are presented in Table 7 together with the data for the same air mass type from Table 2. In both cases, we could see a six-modal structure of the SD. The same modes were present in both cases, even though the modal diameters were somewhat different. The main difference between the two cases was the lower concentration of fine particles — particles in the nucleation and Aitken mode — during the non-event days as compared with that during the event days.

Summary

The most essential conclusions drawn from our investigation are:

— Multivariate statistical methods, such as the factor analysis, are suitable for the determination of the averaged modal structure of the aerosol particle size distribution (SD) because they process a long time series of the SD. In order to improving the fitting, we inserted additional modes in some cases. These modes were not clear in the picture showing factor loadings, but the graph of some factor loading had a small local small maximum at this point of a diameter scale. We treated these maximums as the results of poor statistical material, which does not enable the discovery of an additional factor.

— The modal structure of the particle SD depends essentially on the prehistory of the air mass in which the aerosol properties are being measured.

— The nucleation event days, and especially the hours when the nucleation burst and initial growth of the freshly-born particles occur, were characterized by extremely high concentrations of nucleation mode particles compared with the non-event days. Later (in most cases during the afternoon), particles number concentrations in the nucleation mode decreased and those in the Aitken mode increased. This clearly shows the dynamics of the particle spectrum.

— In the modified continental Arctic air masses, the nucleation bursts seemed to start with

Table 6. Fitted modal parameters for the air mass class P_MC and for two periods (07:00–13:00 and 13:00–18:00).

	07:00–13:00			13:00–18:00		
	N (cm^{-3})	σ_g	D_g (nm)	N (cm^{-3})	σ_g	D_g (nm)
Nucleation	1200	1.73	6.4	200	1.35	5.6
Aitken1	1600	1.40	24	2000	1.45	12
Aitken2	4450	1.52	82	5980	1.49	56
Condensation	20	1.85	420	100	1.27	232
Droplet				10	2.20	400
Coarse1	0.5	3.80	4400	0.5	1.50	1340
Coarse2				0.4	3.30	2600

Table 7. Fitted modal parameters for the air mass class A_MM. The event days and non-event days have been separated.

		Nucleation	Aitken	Condensation	Droplet	Coarse1	Coarse2
Event days	D_g (nm)	10	40	160	500	900	2400
	σ_g	1.50	1.58	1.40	1.25	1.90	4.00
	N (cm^{-3})	1500	5400	300	5	1.6	0.5
Non-event days	D_g (nm)	12	24	122	400	1000	2800
	σ_g	1.46	1.57	1.40	1.37	1.80	4.00
	N (cm^{-3})	475	2100	65	9	2	0.3

some delay in comparison with the modified maritime Arctic and polar air masses.

Acknowledgements: This work was partly supported by the ESF grants 5387 and 6988. The authors wish to thank our colleagues from the Institute of Environmental Physics of the University of Tartu, especially T. Bernotas and A. Mirme, for the help with instrument updating and calibration, and A. Reinart and M. Vana for the valuable recommendations.

References

Birmili W., Wiedensohler A., Heintzenberg J. & Lehmann K. 2001. Atmospheric particle number size distribution in central Europe: Statistical relations to air masses and meteorology. *J. Geophys. Res.* 106: 32005–32018.

Birmili W., Berresheim H., Plass-Dülmer C., Elste T., Gilge S., Wiedensohler A. & Uhrner U. 2003. The Hohenpeissenberg aerosol formation experiment (HAFEX): A long-term study including size-resolved aerosol, H_2SO_4, OH, and monoterpenes measurements. *Atmos. Chem. Phys.* 3: 361–376.

Dal Maso M., Kulmala M., Riipinen I., Wagner R., Hussein T, Aalto P.P. & Lehtinen K.E.J. 2005. Formation and growth rates of fresh atmospheric aerosols: eight years of aerosol size distribution data from SMEAR II, Hyytiälä, Finland. *Boreal Env. Res.* 10: 323–336.

Draxler R.R. & Hess G.D. 1997. *Description of the HYSPLIT_4 modelling system*. NOAA Tech. Memo. ERL ARL-224, Silver Spring, MD.

Draxler R.R. & Hess G.D. 1998. An overview of the HYSPLIT_4 modelling system for trajectories, dispersion and deposition. *Austr. Meteorol. Mag.* 47: 295–308.

Hõrrak U., Tammet H., Aalto P.P. & Kulmala M. 2004. Study of air ions and nanometer particles in the atmosphere during nucleation burst events. *Report Series in Aerosol Science* 71A: 184–189.

Hussein T., Hämeri K., Aalto P.P., Paatero P. & Kulmala M. 2005. Modal structure and spatial-temporal variations of urban and suburban aerosols in Helsinki, Finland. *Atmos. Environ.* 39: 1655–1668.

Kleinbaum D.G., Kupper L.L. & Muller K.E. 1987. *Applied regression analysis and other multivariable methods*. PWS-Kent Publishing Company, Boston.

Korhonen P., Kulmala M., Laaksonen A., Viisanen Y., McGraw R. & Seinfeld J.H. 1999. Ternary nucleation of H_2SO_4, NH_3, and H_2O in the atmosphere. *J. Geophys. Res.* 104: 26349–26353.

Krzanowski W.J. 2000. *Principles of multivariate analysis. A user's perspective*. Oxford University Press Inc., New York.

Kulmala M., Pirjola L. & Mäkelä J.M. 2000. Stable sulphate clusters as a source of new atmospheric particles. *Nature* 404: 66–69.

Kulmala M., Hämeri K., Aalto P.P., Mäkelä J.M., Pirjola L., Nilsson E.D., Buzorius G., Rannik Ü., Dal Maso M., Seidl W., Hoffman T., Janson R., Hansson H.-C., Viisanen Y., Laaksonen A. & O'Dowd C.D. 2001. Overview of the international project on biogenic aerosol formation in the boreal forest (BIOFOR). *Tellus* 53B: 324–343.

Kulmala M. 2003. How particles nucleate and grow. *Science* 302: 1000–1001.

Kulmala M., Vehkamäki H., Petäjä T., Dal Maso M., Lauri A., Kerminen V.-M., Birmili W. & McMurry P.H. 2004a. Formation and growth rates of ultrafine atmospheric particles: a review of observations. *J. Aerosol Sci.* 35: 143–176.

Kulmala M., Laakso L., Lehtinen K.E.J., Riipinen I., Dal Maso M., Anttila T., Kerminen V.-M., Horrak U., Vana M. & Tammet H. 2004b. Initial steps of aerosol growth. *Atmos. Chem. Phys.* 4: 2553–2560.

Laakso L., Anttila T., Lehtinen K.E.J., Aalto P.P., Kulmala M., Hõrrak U., Paatero J., Hanke M. & Arnold F. 2004. Kinetic nucleation and ions in boreal forest particle formation events. *Atmos. Chem. Phys.* 4: 2353–2366.

Lovejoy E.R., Curtius J. & Froyd K.D. 2004. Atmospheric ion-induced nucleation of sulphuric acid and water. *J. Geophys. Res.* 109, D08204, doi:10.1029/2003JD004460.

Meng Z. & Seinfeld J.H. 1994. On the source of the submicrometer droplet mode of urban and regional aerosols. *Aerosol Sci. Tech.* 20: 253–265.

Mäkelä J.M., Aalto P., Jokinen V., Pohja T., Nissinen A., Palmroth S., Markkanen T., Seitsonen K., Lihavainen H. & Kulmala M. 1997. Observations of ultrafine aerosol particle formation and growth in boreal forest. *Geophys. Res. Lett.* 24: 1219–1222.

Mäkelä J.M., Dal Maso M., Pirjola L., Keronen P., Laakso L., Kulmala M. & Laaksonen A. 2000. Characteristics of the atmospheric particle formation events observed at a boreal forest site in southern Finland. *Boreal Env. Res.* 5: 299–313.

O'Dowd C., McFiggans G., Creasey D.J., Pirjola L., Hoell C., Smith M.H., Allan B.J., Plane J.M.C., Heard D.E., Lee J.D., Pilling M.J. & Kulmala M. 1999. On the photochemical production of new particles in the coastal boundary layer. *Geophys. Res. Lett.* 26: 1707–1710.

O'Dowd C.D., Hämeri K., Mäkelä J.M., Pirjola L., Kulmala M., Jennings S.G., Berresheim H., Hansson H.-C., de Leeuw G., Kunz G.J., Allen A.G., Hewitt C.N., Jackson A., Viisanen Y. & Hoffmann T. 2002. A dedicated study of New Particle Formation and Fate in the Coastal Environment (PARFORCE): overview of objectives and achievements. *J. Geophys. Res.* 107(D19), 8108, doi:10.1029/2001JD000555.

Pugatšova A. & Tamm E. 2004. Characteristics of the measurement spectrum of the atmospheric aerosol and particle total concentration depending on air mass origin and its meteorological parameters. In: *Abstracts of the European Aerosol Conference 2004, 6–10 September 2004, Budapest*, Elsevier, pp. 1033–1034.

Pugatšova A., Reinart A. & Tamm E. 2007. Features of the multimodal aerosol size distribution depending on the air mass origin in the Baltic region. *Atmos. Environ.* doi:10.1016/j.atmosenv.2007.01.044. [In press].

Stainer C.O., Khlystov A.Y. & Pandis S.N. 2002. Investi-

gation of nucleation bursts during the Pittsburgh air quality study. In: Wang C.-S. (ed.), *Abstracts of the Sixth International Aerosol Conference, 9–13 September 2002, Taipei, Taiwan, Chinese Association for Aerosol Research in Taiwan,* pp. 1291–1292.

Stevens J. 1996. *Applied multivariate statistics for the social sciences*. Lawrence Erlbaum Associates, Inc., Mahwah, New Jersey.

Tamm E., Hõrrak U., Mirme A. & Vana M. 2001. On the charge distribution on atmospheric nanoparticles. *J. Aerosol Sci*. 32: S347–S348.

Tammet H., Mirme A. & Tamm E. 2002. Electrical aerosol spectrometer of Tartu University. *Atmos. Res*. 62: 315–324.

Tunved P., Hansson H.-C., Kulmala M., Aalto P., Viisanen Y., Karlsson H., Kristensson A., Swietlicki E., Dal Maso M., Ström J. & Komppula M. 2003. One year boundary layer aerosol size distribution data from five Nordic background stations. *Atmos. Chem. Phys*. 3: 2183–2205.

Vana M., Jennings S.G., Kleefeld C., Mirme A. & Tamm E. 2002. Small-particle concentration fluctuations at a coastal site. *Atmos. Res*. 63: 247–269.

Vana M., Kulmala M., Dal Maso M., Horrak U. & Tamm E. 2004. Comparative study of nucleation mode aerosol particles and intermediate air ions formation events at three sites. *J. Geophys. Res*. 109, D17201, doi:10.1029/2003JD004413.

Vana M., Tamm E., Hõrrak U., Mirme A., Tammet H., Laakso L., Aalto P.P. & Kulmala M. 2006. Charging state of atmospheric nanoparticles during the nucleation burst events. *Atmos. Res*. 82: 536–546.

Väkevä M., Hämeri K., Puhakka T., Nilsson E.D., Hohti H. & Mäkelä J.M. 2000. Effects of meteorological processes on aeroso areal particle size distribution in an urban background. *J. Geophys. Res*. 105: 9807–9821.

Whitby K.T. & Sverdrup G.M. 1978. The physical characteristics of sulphur aerosols. *Atmos. Environ*. 12: 135–159.

Woo K.S., Chen D.R., Pui D.Y.H. & McMurry P.H. 2001. Measurements of Atlanta aerosol size distributions: observations of ultrafine particle events. *Aerosol Sci. Tech*. 34: 75–87.

Yu F. & Turco R.P. 2001. From molecular clusters to nanoparticles: role of ambient ionization in tropospheric aerosol formation. *J. Geophys. Res*. 106: 4797–4814.